

Frame Isotropic Multiresolution Analysis for Micro CT Scans of Coronary Arteries

Alex Gittens, Bernhard Bodmann, Manos Papadakis, and Donald Kouri

1. Introduction

The presence of vulnerable plaques—lipid pools capped by fibrous tissues—near the arterial lumen has been associated with an increased risk of acute myocardial infarction. Current relevant medical imaging modalities are primarily aimed at the detection of calcific deposits, but the presence of vulnerable plaques, particularly those in an early stage of development, is not directly associated with the presence of calcific deposits. Therefore, a new imaging technique for early noninvasive detection of vulnerable plaques is of interest.

The objective of this work was to develop a texture-based algorithm for semi-automated tissue type discrimination in high-resolution CT scans, with the following properties:

1. It should operate on the entire three dimensional volume of CT data.
2. Features and textures should be identified regardless of their orientation.
3. The output of the algorithm should be unambiguous: different tissue types should have consistent signatures.

The second desired property is unrealizable with the commonly used tensor product constructions, due to the directional biases introduced in their construction. To avoid introducing such preferences, and to minimize the computational requirements imposed by the first goal, we use fast wavelet transforms based on a novel non-separable frame MRA we call the First Generation Isotropic MRA.

2. First Generation Isotropic MRA

The First Generation IMRA is constructed by taking the GFMRA comprising the family of increasing closed subspaces $\{V_j\}$, defined to be the set of functions in $L^2(\mathbb{R}^n)$ whose Fourier transforms vanish outside of $2^j\mathbb{B}$, where $\mathbb{B} = \{\xi \in \mathbb{R}^n : |\xi| \leq b_0\}$ is the closed ball of radius $\frac{1}{4} < b_0 < \frac{1}{2}$. With this choice, we obtain invariance of the spaces V_j and W_j under rotation:

Theorem 1. Each V_j is invariant under any rotation about any center $x \in \mathbb{R}^n$. The same is true for each detail space $W_j = V_{j+1} \cap V_j^\perp$, $j \in \mathbb{Z}$.

We take the frame scaling function to be ϕ where $\hat{\phi} = \chi_{\mathbb{B}}$, so $\{T_k\phi : k \in \mathbb{Z}^n\}$ is a Parseval frame for V_0 , and obtain the frame wavelets

$$\psi_i(\xi) = 2^{-\frac{n}{2}} e^{i\pi \langle \mathbf{q}_i, \xi \rangle} \chi_{\mathbb{S}}\left(\frac{\xi}{2}\right),$$

where \mathbb{S} is the spherical shell with inner radius b_0 and outer radius $2b_0$, and $\{\mathbf{q}_i : i = 0, 1, \dots, 2^n - 1\}$ are representatives of the quotient group $\mathbb{Z}^n/2(\mathbb{Z}^n)$.

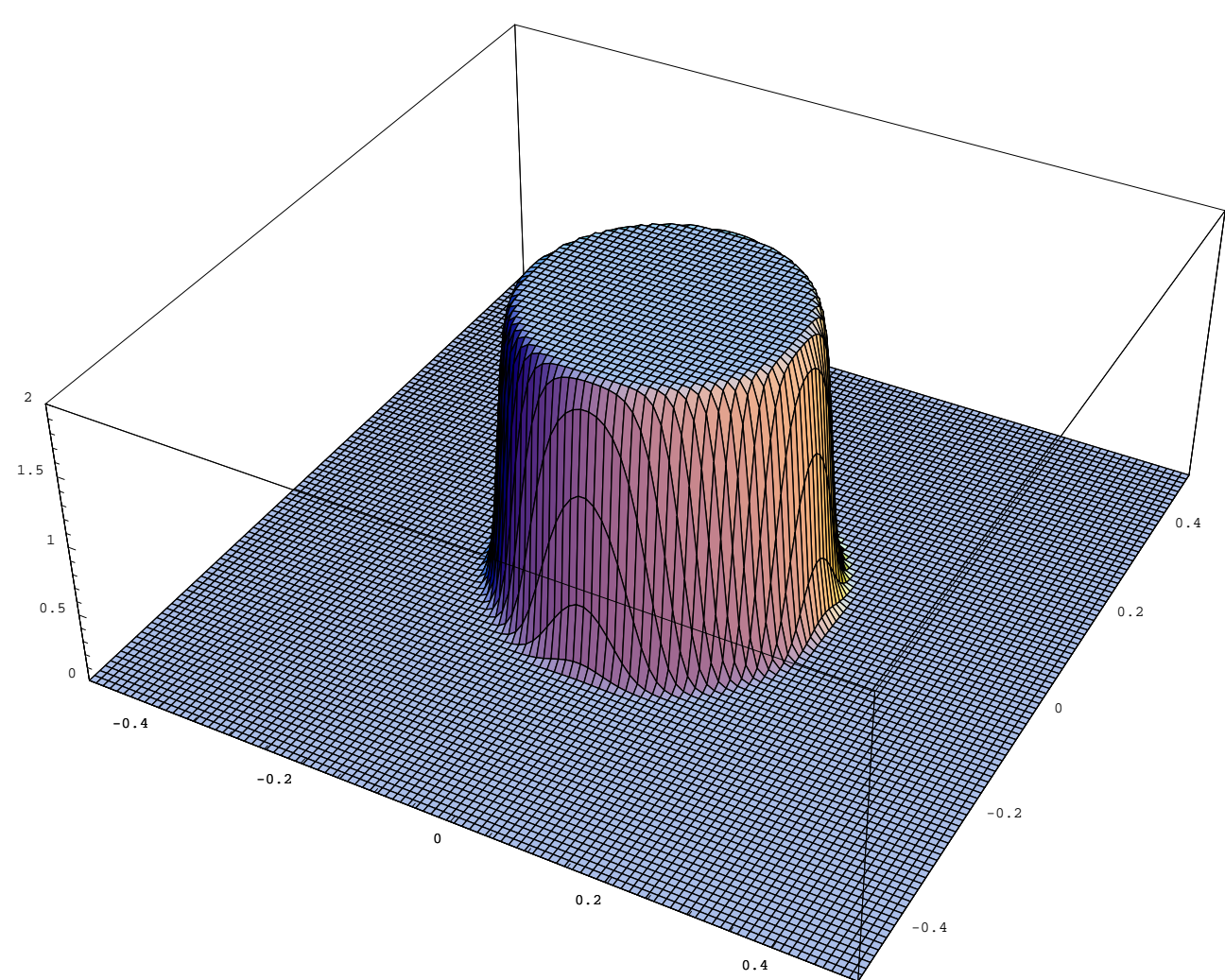


Figure 1: Isotropic low-pass filter derived from the two-dimensional First Generation IMRA.

The First Generation IMRA gives rise to fast wavelet algorithms similar to those associated with separable MRAs. From the fact that $\mathbb{B} \subset \mathbb{T}^n$, we have

Theorem 2. If $f \in V_0$, then

$$f = \sum_{k \in \mathbb{Z}^n} f(k) T_k \phi,$$

where the right-hand side converges in the L^2 -norm and uniformly if $f \in V_0$ is continuous,

which shows that the input of the fast wavelet algorithms resulting from the First Generation IMRA consists of the samples of the input digital image on \mathbb{Z}^n . To implement the decomposition algorithm, we use two channels, a low and a high. Signals passed through these channels are filtered by the appropriate analysis filters; the output of the low channel is decimated, while the output of the high channel remains undecimated. The reconstruction algorithm is implemented analogously by means of the corresponding synthesis filters.

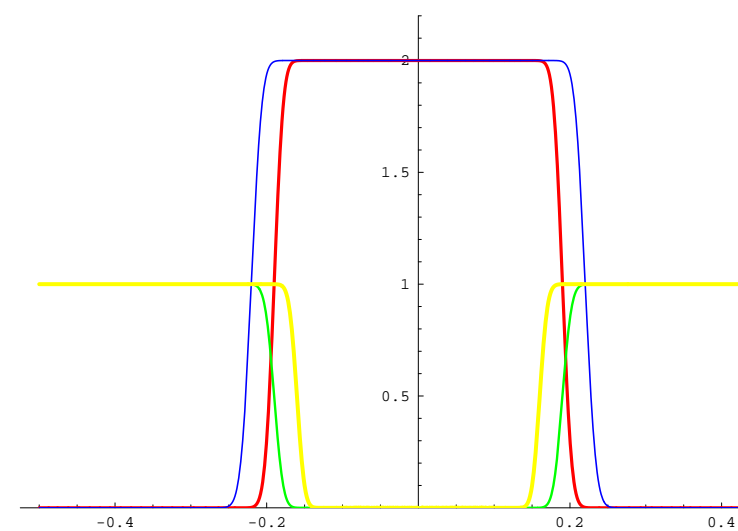


Figure 2: Cross-section of the radial analysis and synthesis filters associated with the two-dimensional First Generation IMRA: the synthesis filters have larger frequency support than the analysis filters. We refer to the use of radial analysis filters with smaller bandwidth than their synthesis counterparts as radial oversampling.

To achieve improved localization properties we used smoothed approximations of the ideal low and high pass filters (see Figure 1). We designed these filters so the pass band of the synthesis filters is the aggregate of the pass and transition bands of the analysis filter (see Figure 2). In this type of filter design, which we refer to as radial oversampling, the synthesis filters serve as “duals” of their analysis counterparts, facilitating exact reconstruction.

3. Tissue Types

Under the hypothesis that there are finitely many types of tissue (viz., lumen, calcified, lipid, fibrous, and muscular), we modeled our CT images as disjoint unions of regions each comprising one type of tissue. We characterize tissues by their correlations and means, and account for multiple levels of resolutions. Formally, we stipulate a tissue of one type, at a fixed scale, to be a wide sense homogenous, isotropic discrete random field whose first and second moments can be obtained by averaging a tissue sample over all shifts.

Definition 1. A tissue type τ at resolution level j is a family of real-valued variables over some probability space $(\Omega, \mathbb{P}, \mathcal{F})$ with the following properties:

1. *Spatial homogeneity:* $\mathbb{E}[\tau_k] = \bar{\tau}$ is independent of k , and the correlation of any two random variables τ_k and $\tau_{k'}$ depends only on $k - k'$.
2. *Special Property 1:* Given G , a filter with absolutely summable taps, the mean value of the filtered process $(G * \tau_k)$ equals the limit of the average

$$\frac{1}{|\mathbb{V}|} \sum_{k \in \mathbb{V}} (G * \tau)_{k+k}$$

as $\mathbb{V} \nearrow \mathbb{Z}^n$ ($|\mathbb{V}|$ is the number of indices in \mathbb{V}).

3. *Special Property 2:* The approximations

$$C_{k,k'}(\mathbb{V}) = \frac{1}{|\mathbb{V}|} \sum_{l \in \mathbb{V}} (\tau_{k+l} - \bar{\tau}_k(\mathbb{V})) (\tau_{k'+l} - \bar{\tau}_{k'}(\mathbb{V})),$$

where $\tau_k(\mathbb{V})$ is the local average of $\{\tau_{k'} : k' \in \mathbb{V}\}$ over \mathbb{V} , converge to the covariance matrix.

4. *Special Property 3:* For each $k, k' \in \mathbb{Z}^n$ and every summable filter G ,

$$\lim_{\mathbb{V} \nearrow \mathbb{Z}^n} (G * C(\mathbb{V}) G)_{k,k'} = (G * C G)_{k,k'}.$$

As a consequence of this definition, tissues are preserved by linear filtering:

Theorem 3. The properties of a tissue type at resolution level j are preserved by convolution with a summable filter G .

Therefore, lowpass filtering and then downsampling a tissue of type τ at resolution level j produces a corresponding tissue type at resolution level $j - 1$.

Another consequence of the definition of a tissue is that the statistics of a tissue type can be determined by applying Special Properties 1 and 2. Furthermore, it is possible to fit a least squares predictive filter to a given tissue type, with the property that in the limit of arbitrarily large training sets the filter becomes a least squares estimator for the tissue with respect to the probability measure associated with τ .

Theorem 4. Let τ be a tissue at resolution level j , and P be a prediction filter of a fixed length that minimizes $Q(P - I)$, the mean-square error given by

$$Q(P - I) = \mathbb{E}[(P - I)^*(\tau - \bar{\tau})]_k^2 = ((P - I)^* C (P - I))_{k,k}.$$

Fix $k \in \mathbb{Z}^n$ and choose for each $\mathbb{V} \subset \mathbb{Z}^n$ a prediction filter $P(\mathbb{V})$ of the same length that minimizes $Q_{\mathbb{V},k}(P(\mathbb{V}) - I)$, the locally averaged mean-square error over \mathbb{V} . Then

$$\lim_{\mathbb{V} \nearrow \mathbb{Z}^n} Q(P(\mathbb{V}) - I) = Q(P - I).$$

From the previous two theorems, we see that filters can be optimized separately over each subband. Since these filters encode the statistics of the tissue they are optimized over, they can be used as the basis of a non-parametric statistical test for determining whether a given sample is of that type of tissue.

4. Algorithm: Tissue Discrimination

1. Select a reference region of normal tissue from the sample.
2. Decompose the reference region into three subbands ρ_i , $i \in \{1, 2, 3\}$.
3. LMSE fit a predictive filter F_i to each subband of the reference region, and calculate the root mean squared errors σ_i .
4. Decompose the sample into three subbands S_i .
5. Calculate the error images $\epsilon_i = S_i - F_i(S_i)$.
6. In each subband, isolate the abnormal tissue \bar{S}_i :

$$\bar{S}_i(x, y, z) = \begin{cases} S_i(x, y, z) & \text{if } |\epsilon_i(x, y, z)| > 3\sigma_i, \\ 0 & \text{otherwise} \end{cases}$$

7. Reconstruct, from the subbands \bar{S}_i , a volume representing the abnormal tissue in the sample.

5. Discussion

The results of running our algorithm on two slices of a CT volume scan of a coronary artery are shown below.

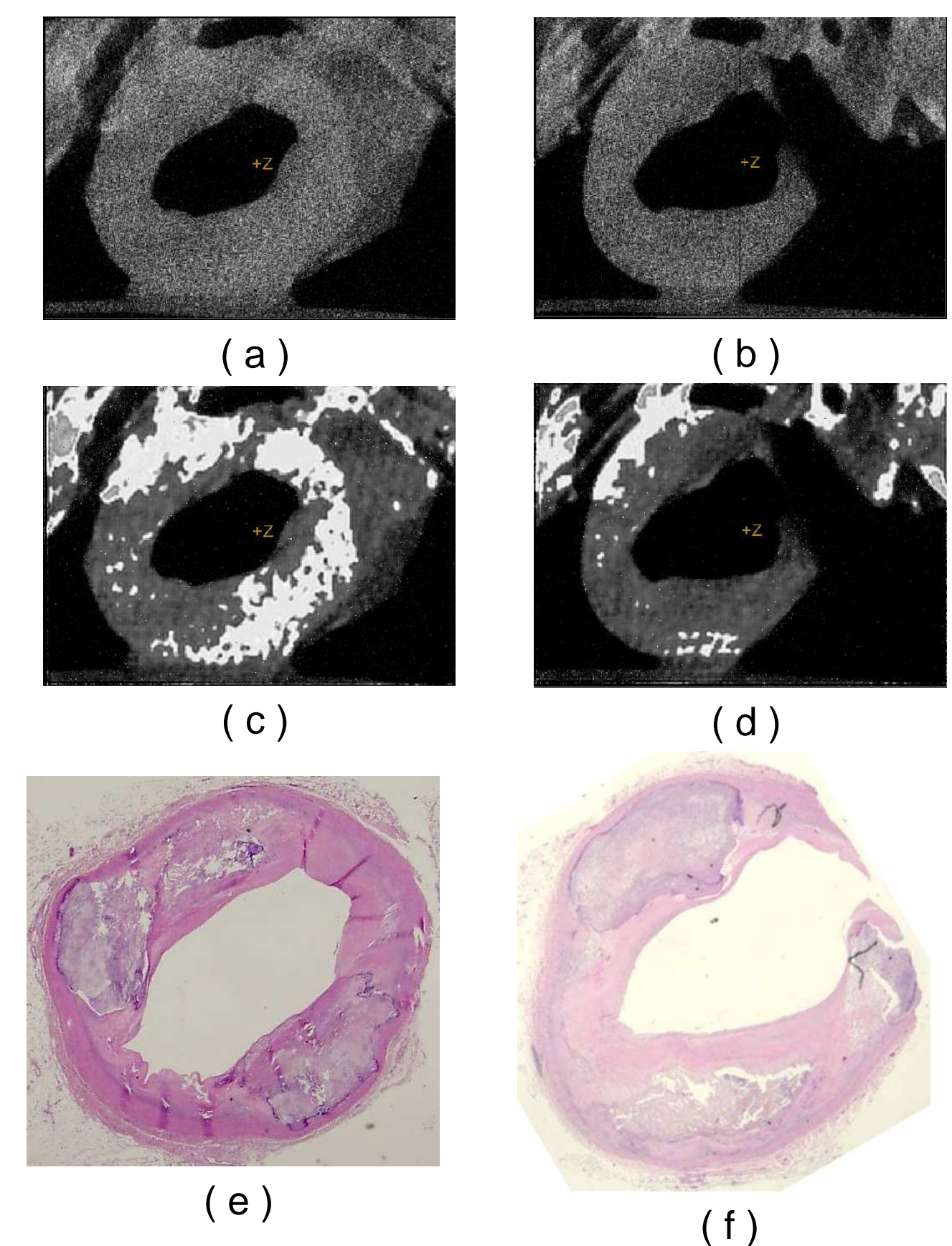


Figure 3: (a) and (b) are slices of CT scans of coronary artery specimens taken using a General Electric RS-9 Micro CT scanner with a linear resolution of 27 micrometers; (c) and (d) are corresponding slices in the respective processed volumes; (e) and (f) are corresponding slices of the arteries, obtained for histological comparison after the scans were taken—the gray regions embedded in the artery wall in these images are pools of lipid.

As demonstrated by the detection of the lipid pools in Figure 3, our algorithm is capable of indicating the presence of anomalous tissues not visible in the unprocessed CT volume.

A collection of coronary artery datasets has been processed with our tissue discrimination algorithm, using the Fast Wavelet transform associated with the First Generation Isotropic MRA; we are in the process of using the results to systematically examine its accuracy, in terms of the number of features it correctly detects, and the robustness of its output as the reference tissue region is changed.

References

- [1] B. Bodmann and et. al. Frame Isotropic Multiresolution Analysis for Micro Ct Scans of Coronary Arteries. In M. Papadakis, A. Laine, and M. Unser, editors, *Wavelets XI*, volume 5914 of *Proceedings SPIE*, 2005.
- [2] M. Papadakis, G. Gogoshin, I.A. Kakadiaris, D.J. Kouri, and D.K. Hoffman. Non-separable radial frame multiresolution analysis in multidimensions. *Numer. Function. Anal. Optimization*, 24:907–928, 2003.